Covariance Statistics of Fully Polarimetric Brightness Temperature Measurements

Jinzheng Peng, *Member, IEEE*, and Christopher S. Ruf, *Fellow, IEEE*

***Abstract*—The covariance statistics of measurements by a fully polarimetric microwave radiometer are derived using a fundamental noise-theoretic approach. Previous published derivations of a similar nature have only included the third Stokes brightness temperature. The results are confirmed by a series of numerical Monte Carlo simulations of the underlying radiometric measurement process. It is found that the additive noise that is present in the measurements can be correlated between polarimetric channels and that the correlation statistics will vary as a function of the polarization state of the scene under observation. General expressions are also derived for the measurement precision (the radiometric NEΔT) and the system noise temperature of the third and fourth Stokes channels. It is found that both the precision and noise temperature can also depend on the polarization state of the scene.**

***Index Terms*—Microwave radiometry, noise measurements, polarimetry.**

I. Introduction

A FULLY polarimetric microwave radiometer measures the complex correlation between vertically and horizontally polarized microwave radiation from the scene under observation [10]. The radiation can be described by the modified Stokes parameters in brightness temperature (TB) under the Rayleigh–Jeans approximation [1]. Two approaches to measure the Stokes parameters, namely, coherent and incoherent detection [2], are commonly adopted by fully polarimetric radiometers.

A coherent-detection radiometer measures the complex covariance of the v- and h-pol components of the signal directly using a complex multiplier [3]. The resulting polarimetric components of T_B are designated T_3 and T_4 for the real and imaginary components of correlation, respectively. In comparison to a coherent-detection radiometer, an incoherent-detection radiometer most often measures the $\pm 45^\circ$ slant linear and left- and right-hand circular polarization components of the TB (resulting in T_P, T_M, T_L, and T_R, respectively) in addition to the vertical and horizontal components, i.e., T_v, and T_h, respectively. Incoherent-detection radiometers often use hybrid couplers to form the necessary polarization channels [4]–[6]. T_3 and T_4 are derived as the difference between T_P and T_M, and the difference between T_L and T_R, respectively.

Manuscript received October 20, 2009; revised December 8, 2009. Date of publication February 5, 2010; date of current version April 29, 2010.

The authors are with the Space Physics Research Laboratory, Department of Atmospheric, Oceanic and Space Sciences, University of Michigan, Ann Arbor, MI 48109 USA (e-mail: cruf@umich.edu).

Color versions of one or more of the figures in this paper are available online at http://ieeexplore.ieee.org.

Digital Object Identifier 10.1109/LGRS.2009.2039115

In order to determine the measurement precision of the third and fourth Stokes parameters, the covariance statistics of the radiometer measurements are needed. In our previous work [8], we examined the covariance behavior of the noise associated with measurement of the third Stokes channel. That work is expanded here to include the fourth Stokes channel. We consider the correlation between the noise in the fourth Stokes channel and that of each of the other channels. We also develop a general expression for the NEΔT precision of the fourth Stokes measurement. Finally, a numerical Monte Carlo simulation is performed, which directly estimates the covariance between the measurement noise in the different polarimetric channels. Those estimates confirm the general expressions that have been developed.

II. Statistics of Radiometer Measurements

A. Noise Covariance of an Incoherent-Detection Hybrid Combining Polarimetric Radiometer

The signal flow through a hybrid combining fully polarimetric microwave radiometer is shown in Fig. 1. In the figure, G_p represents the channel gain in channel p, and B is the bandwidth (assumed the same in the v- and h-pol channels). The amplified and filtered signal $v_p(t)$ can be written as the sum of an external thermal noise signal that is incident on the radiometer and internal receiver noise, or

$$\begin{aligned} v_v(t) &= \sqrt{G_v}\,[b_v(t) + n_v(t)] \\ v_h(t) &= \sqrt{G_h}\,[b_h(t) + n_h(t)] \end{aligned} \tag{1}$$

where $b_p(t)$ is the time-varying noise voltage at polarization p associated with the TB (see [9] for a detailed definition). The noise voltage is linearly proportional to the incident electric field associated with that TB and has units of $\mathrm{K}^{-1/2}$. $b_p(t)$ is the noise voltage in receiver channel p. Both $b(t)$ and $n(t)$ are modeled as additive zero-mean band-limited Gaussian-distributed random variables. The auto- and cross-correlation relationships between the voltages associated with the TB are given by [9]

$$\langle b_v(t) b_v(t-\tau)\rangle = T_v \cos(2\pi f_c \tau)\mathrm{sinc}(B\tau) \tag{2a}$$

$$\langle b_h(t) b_h(t-\tau)\rangle = T_h \cos(2\pi f_c \tau)\mathrm{sinc}(B\tau) \tag{2b}$$

$$\langle b_v(t) b_h(t-\tau)\rangle = \left\{ \frac{T_3}{2}\cos(2\pi f_c \tau) - \frac{T_4}{2}\sin(2\pi f_c \tau) \right\} \times \mathrm{sinc}(B\tau) \tag{2c}$$

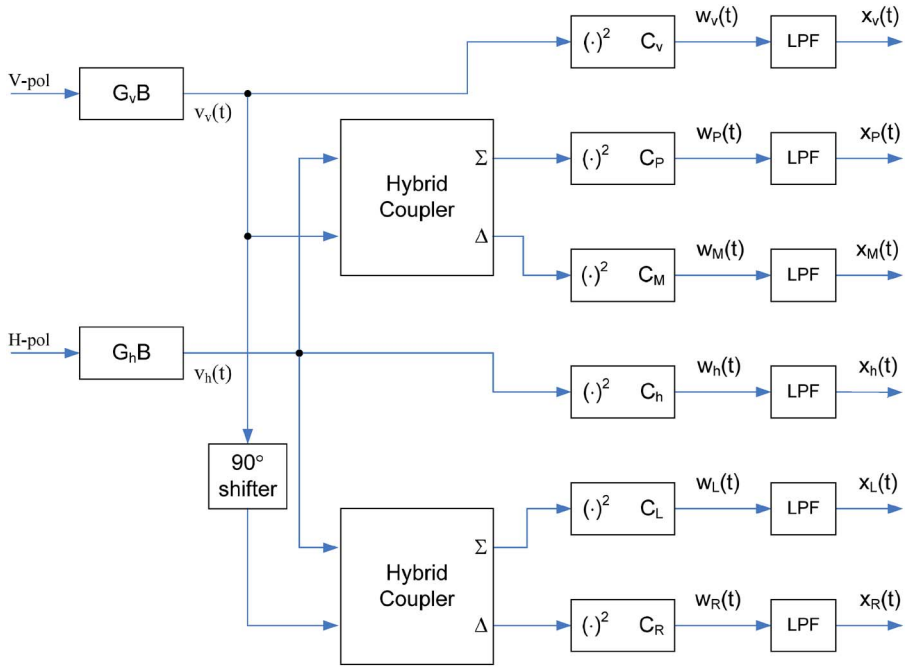

Fig. 1. Signal-flow diagram for a hybrid combining polarimetric microwave radiometer. Subscripts v, h, P, M, L, and R designate the vertical, horizontal, $\pm 45^\circ$ slant linear, and left- and right-hand circular polarization channels, respectively.

where f_c is the center frequency of the signal and $\mathrm{sinc}(u) = \sin(\pi u)/(\pi u)$. The variance and covariance of the signals are found by evaluating the autocorrelations in (2) at $\tau = 0$. The variance of $n(t)$ is similarly related to the receiver noise temperature by

$$\langle n_v^2(t)\rangle = T_{Rv} \quad \langle n_h^2(t)\rangle = T_{Rh} \tag{3}$$

where T_{Rv} and T_{Rh} are the noise temperatures of the v- and h-pol receivers. $n_v(t)$ and $n_h(t)$ are uncorrelated.

A hybrid combining polarimetric radiometer forms $\pm 45^\circ$ slant linear and left- and right-hand circular polarized channels from $v_v(t)$ and $v_h(t)$ by summing and differencing them in hybrid couplers, as shown in Fig. 1. The signals from these channels, as well as the original signals, are then passed through square-law detectors with sensitivity c_x ($x = v, P, M, h, L,$ and R). The time integration of the six signals is modeled as an ideal "top-hat" low-pass filter (LPF) with bandwidth τ^{-1}, where τ is the integration time. The six output polarization signals are $x_v(t)$, $x_P(t)$, $x_M(t)$, $x_h(t)$, $x_L(t)$, and $x_R(t)$. The expected value of these signals (i.e., the dc component of their spectra) is proportional to the six associated TBs. The variance of the signals (i.e., the integral over the ac component of their spectra) represents the additive noise that is present in the measurements [7].

The correlation coefficients between the signal pairs of polarization channels v, P, M, and h are described in [8]. The correlation coefficients between signal pairs that include the L and R channels are derived here in a similar manner as

$$\rho_{v,L} = \frac{\left(T_{\mathrm{sys},v} + \frac{\sqrt{g}}{2}T_4\right)^2 + \frac{g}{4}T_3^2}{T_{\mathrm{sys},v}\cdot(T_{\mathrm{sys},v} + gT_{\mathrm{sys},h} + \sqrt{g}T_4)} \tag{4a}$$

$$\rho_{v,R} = \frac{\left(T_{\mathrm{sys},v} - \frac{\sqrt{g}}{2}T_4\right)^2 + \frac{g}{4}T_3^2}{T_{\mathrm{sys},v}\cdot(T_{\mathrm{sys},v} + gT_{\mathrm{sys},h} - \sqrt{g}T_4)} \tag{4b}$$

$$\rho_{P,L} = \frac{\left[T_{\mathrm{sys},v} + \frac{\sqrt{g}}{2}(T_3+T_4)\right]^2 + \left[gT_{\mathrm{sys},h} + \frac{\sqrt{g}}{2}(T_3+T_4)\right]^2}{(T_{\mathrm{sys},v} + gT_{\mathrm{sys},h} + \sqrt{g}T_3)\cdot(T_{\mathrm{sys},v} + gT_{\mathrm{sys},h} + \sqrt{g}T_4)} \tag{4c}$$

$$\rho_{P,R} = \frac{\left[T_{\mathrm{sys},v} + \frac{\sqrt{g}}{2}(T_3-T_4)\right]^2 + \left[gT_{\mathrm{sys},h} + \frac{\sqrt{g}}{2}(T_3-T_4)\right]^2}{(T_{\mathrm{sys},v} + gT_{\mathrm{sys},h} + \sqrt{g}T_3)\cdot(T_{\mathrm{sys},v} + gT_{\mathrm{sys},h} - \sqrt{g}T_4)} \tag{4d}$$

$$\rho_{M,L} = \frac{\left[T_{\mathrm{sys},v} - \frac{\sqrt{g}}{2}(T_3-T_4)\right]^2 + \left[gT_{\mathrm{sys},h} - \frac{\sqrt{g}}{2}(T_3-T_4)\right]^2}{(T_{\mathrm{sys},v} + gT_{\mathrm{sys},h} - \sqrt{g}T_3)\cdot(T_{\mathrm{sys},v} + gT_{\mathrm{sys},h} + \sqrt{g}T_4)} \tag{4e}$$

$$\rho_{M,R} = \frac{\left[T_{\mathrm{sys},v} - \frac{\sqrt{g}}{2}(T_3+T_4)\right]^2 + \left[gT_{\mathrm{sys},h} - \frac{\sqrt{g}}{2}(T_3+T_4)\right]^2}{(T_{\mathrm{sys},v} + gT_{\mathrm{sys},h} - \sqrt{g}T_3)\cdot(T_{\mathrm{sys},v} + gT_{\mathrm{sys},h} - \sqrt{g}T_4)} \tag{4f}$$

$$\rho_{h,L} = \frac{\left(gT_{\mathrm{sys},h} + \frac{\sqrt{g}}{2}T_4\right)^2 + \frac{g}{4}T_3^2}{gT_{\mathrm{sys},h}\cdot(T_{\mathrm{sys},v} + gT_{\mathrm{sys},h} + \sqrt{g}T_4)} \tag{4g}$$

$$\rho_{h,R} = \frac{\left(gT_{\mathrm{sys},h} - \frac{\sqrt{g}}{2}T_4\right)^2 + \frac{g}{4}T_3^2}{gT_{\mathrm{sys},h}\cdot(T_{\mathrm{sys},v} + gT_{\mathrm{sys},h} - \sqrt{g}T_4)} \tag{4h}$$

$$\rho_{L,R} = \frac{(T_{\mathrm{sys},v} - gT_{\mathrm{sys},h})^2 + gT_3^2}{(T_{\mathrm{sys},v} + gT_{\mathrm{sys},h} + \sqrt{g}T_4)\cdot(T_{\mathrm{sys},v} + gT_{\mathrm{sys},h} - \sqrt{g}T_4)} \tag{4i}$$

where $g = G_h/G_v$ is the ratio of h-pol-to-v-pol channel gain. $T_{\mathrm{sys},v} = T_v + T_{Rv}$ and $T_{\mathrm{sys},h} = T_h + T_{Rh}$ are the system

noise temperatures of the v- and h-pol channels, respectively. Note that the correlation coefficients are independent of bandwidth (B) and integration time (τ).

The NEΔT of each channel is given by

$$\Delta T_v = \frac{T_{\mathrm{sys},v}}{\sqrt{B\tau}} = \frac{T_v + T_{Rv}}{\sqrt{B\tau}} \tag{5a}$$

$$\Delta T_P = \frac{T_{\mathrm{sys},P}}{\sqrt{B\tau}} = \frac{1}{\sqrt{B\tau}} \cdot \frac{T_{\mathrm{sys},v} + gT_{\mathrm{sys},h} + \sqrt{g}T_3}{2\sqrt{g}} \tag{5b}$$

$$\Delta T_M = \frac{T_{\mathrm{sys},M}}{\sqrt{B\tau}} = \frac{1}{\sqrt{B\tau}} \cdot \frac{T_{\mathrm{sys},v} + gT_{\mathrm{sys},h} - \sqrt{g}T_3}{2\sqrt{g}} \tag{5c}$$

$$\Delta T_h = \frac{T_{\mathrm{sys},h}}{\sqrt{B\tau}} = \frac{T_h + T_{Rh}}{\sqrt{B\tau}} \tag{5d}$$

$$\Delta T_L = \frac{T_{\mathrm{sys},L}}{\sqrt{B\tau}} = \frac{1}{\sqrt{B\tau}} \cdot \frac{T_{\mathrm{sys},v} + gT_{\mathrm{sys},h} + \sqrt{g}T_4}{2\sqrt{g}} \tag{5e}$$

$$\Delta T_R = \frac{T_{\mathrm{sys},R}}{\sqrt{B\tau}} = \frac{1}{\sqrt{B\tau}} \cdot \frac{T_{\mathrm{sys},v} + gT_{\mathrm{sys},h} - \sqrt{g}T_4}{2\sqrt{g}}. \tag{5f}$$

B. Noise Covariance of a Coherent-Detection Correlating Polarimetric Radiometer

The signal flow through a coherent-detection correlating polarimetric radiometer is shown in Fig. 2. Signals $v_v(t)$, $v_h(t)$, $n_v(t)$, $n_h(t)$, $b_v(t)$, and $b_h(t)$ and their correlation statistics are identical to those in Section II-A. The procedure followed to derive the covariance relationships between the four output signals is similar to that for the hybrid combining radiometer. The correlation coefficient between outputs $x_v(t)$, $x_3(t)$, $x_4(t)$, and $x_h(t)$ can be expressed as follows:

$$\rho_{v,3} = \rho_{3,h} = \frac{\sqrt{2}T_3}{\sqrt{4T_{\mathrm{sys},v}T_{\mathrm{sys},h} + (T_3^2 - T_4^2)}} \tag{6a}$$

$$\rho_{v,4} = \rho_{4,h} = \frac{\sqrt{2}T_4}{\sqrt{4T_{\mathrm{sys},v}T_{\mathrm{sys},h} - (T_3^2 - T_4^2)}} \tag{6b}$$

$$\rho_{v,h} = \frac{T_3^2 + T_4^2}{4T_{\mathrm{sys},v}T_{\mathrm{sys},h}} \tag{6c}$$

$$\rho_{3,4} = \frac{2T_3T_4}{\sqrt{16T_{\mathrm{sys},v}^2T_{\mathrm{sys},h}^2 - (T_3^2 - T_4^2)^2}}. \tag{6d}$$

The NEΔT of each channel is given by

$$\Delta T_v = \frac{T_{va} + T_{R1}}{\sqrt{B\tau}} \tag{7a}$$

$$\Delta T_3 = \sqrt{\frac{4T_{\mathrm{sys},v}T_{\mathrm{sys},h} + (T_3^2 - T_4^2)}{2B\tau}} \tag{7b}$$

$$\Delta T_4 = \sqrt{\frac{4T_{\mathrm{sys},v}T_{\mathrm{sys},h} - (T_3^2 - T_4^2)}{2B\tau}} \tag{7c}$$

$$\Delta T_h = \frac{T_{ha} + T_{R2}}{\sqrt{B\tau}}. \tag{7d}$$

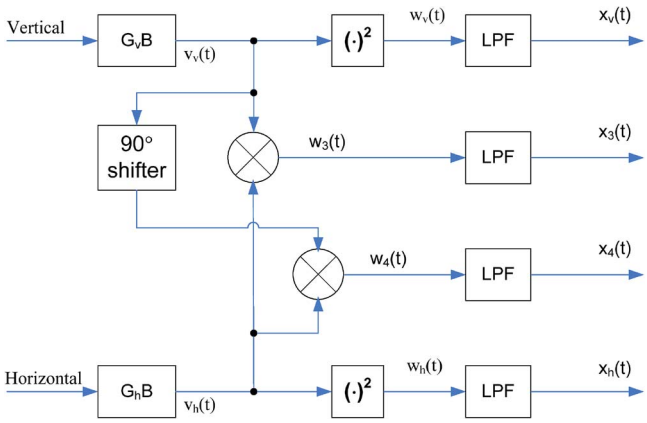

Fig. 2. Signal-flow diagram for a correlating polarimetric microwave radiometer.

C. Application—The Third and Fourth Stokes TBs With a Hybrid Combining Radiometer

The third and fourth Stokes TBs can be computed from the measurements made by a hybrid combining polarimetric radiometer. A general expression for the computation is given by

$$T_3 = [\,2n+1 \quad 2n+1 \quad -2n \quad -2(n+1) \quad 0 \quad 0\,] \times [\,T_v \quad T_h \quad T_P \quad T_M \quad T_L \quad T_R\,]^{\mathrm{t}} \tag{8a}$$

$$T_4 = [\,2n+1 \quad 2n+1 \quad 0 \quad 0 \quad -2n \quad -2(n+1)\,] \times [\,T_v \quad T_h \quad T_P \quad T_M \quad T_L \quad T_R\,]^{\mathrm{t}} \tag{8b}$$

where n can be any real number. The special case $n = -0.5$ produces the most commonly used relationships, i.e., $T_3 = T_P - T_M$ and $T_4 = T_L - T_R$. The three alternative methods considered in [3] to obtain the third and fourth Stokes TBs are special cases of (8) with $n = -0.5, 0,$ and -1.

Equation (8) describes the linear mapping from six incoherent-detection measurements to four polarimetric TBs. By combining this mapping with the full covariance matrix for the six measurements, a general expression for the covariance of the four polarimetric TBs is determined. In particular, if the sensitivities of all the detectors are the same, the covariance is found to be independent of the value of n. In this case, the standard deviations of the additive noise in T_3 and T_4 are given by

$$\Delta T_3 = \sqrt{\frac{4T_{\mathrm{sys},v}T_{\mathrm{sys},h} + (T_3^2 - T_4^2)}{2B\tau}} \tag{9a}$$

$$\Delta T_4 = \sqrt{\frac{4T_{\mathrm{sys},v}T_{\mathrm{sys},h} - (T_3^2 - T_4^2)}{2B\tau}}. \tag{9b}$$

III. Simulation Verification of Covariance Relationship

A computer simulator has been developed to produce realizations of the coherent-detection output signals, namely, $x_v(t)$, $x_3(t)$, $x_4(t)$, and $x_h(t)$ in Fig. 2, from numerically generated realizations of the input signals, namely, $v_v(t)$ and $v_h(t)$. The

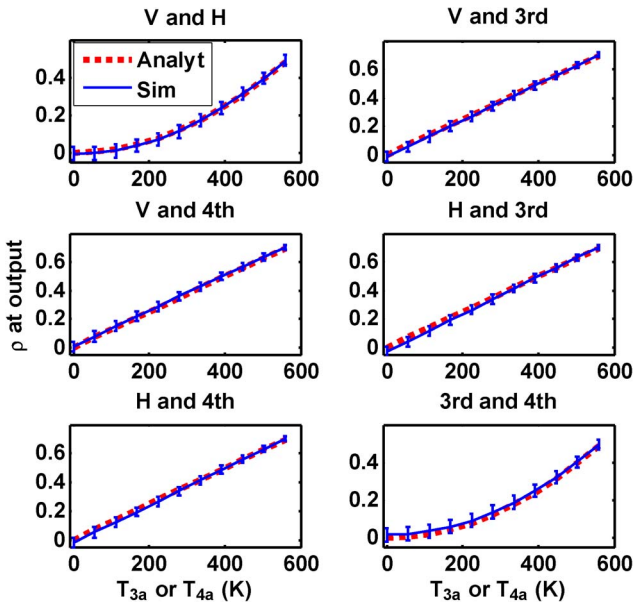

Fig. 3. Correlation between the additive noise in T_v and T_h, T_v and T_3, T_v and T_4, T_h and T_3, T_h and T_4, and T_3 and T_4 as a function of T_3 or T_4 ($T_3 = T_4$ in each case). The red dotted lines plot the analytical expressions, which are derived in Sections II-B and C. The blue solid lines are the empirical results of a Monte Carlo simulation using 1000 independent trials. The error bars represent the standard deviation of these trials.

input signals are generated with the appropriate band-limited Gaussian-distributed noise statistics. The signal flow is modeled, as shown in Fig. 2. Given an assumed partial correlation state for the input signals, this simulator will produce one realization of the radiometer measurement. Repeated independent trials of the simulator are performed to produce a population of measurements from which their covariance relationships can be derived empirically. This Monte Carlo simulation provides an independent means of verifying the correlation relationships given by (6), which were derived analytically.

In the simulations, the uncorrelated receiver noise temperatures are assumed to be 182 and 160 K for the v- and h-pol channels, respectively. The bandwidth of the bandpass filters is 500 MHz, and the 90° phase shifter is implemented by an ideal Hilbert transformer. The input first and second Stokes parameters are set at 390 and 400 K, respectively, and the third and fourth Stokes parameters are varied by adjusting the correlation coefficient magnitude in ten uniformly spaced steps from zero to one. The correlation coefficient phase is set to 45°, so that the third and fourth Stokes parameters are equal.

For each value of the correlation coefficient, 1000 simulated measurements of T_v, T_h, T_3, and T_4 were generated. Empirical covariance statistics were estimated from this population. The results are shown in Fig. 3, which shows the average correlation between the noise in T_v, T_h, T_3, and T_4 as a function of T_3 (or T_4). The error bars in the plots represent the standard deviation of the 1000 trials. The correlation values that are predicted by theory are also plotted for comparison. The predicted and simulated correlations agree closely, with correlation rising monotonically as a function of T_3 or T_4. Note, for example, that the measurement noise in T_v and T_h and that in T_3 and T_4 are largely uncorrelated when the values of T_3 and T_4 are low (i.e., when T_v and T_h are essentially unpolarized). The correlation between any of the pairs: T_v and T_3, T_v and T_4, T_h and T_3, and T_h and T_4, on the other hand, begins to rise immediately as T_3 and T_4 begin to increase.

IV. Conclusion

The covariance statistics of the additive noise component of fully polarimetric radiometer measurements with coherent and incoherent detection have been derived analytically, and the resulting relationships have been verified by numerical simulation. It is found that the noise can be correlated among polarimetric channels and that the correlation statistics will vary as a function of the polarization state of the scene under observation.

The precision obtained from the two detection approaches has been compared. It is found that the two approaches have similar performance, provided that all of the square-law detectors are the same in the radiometer with incoherent detection. This is true for the entire family of possible algorithms by which T_3 and T_4 can be derived from the incoherent-detection measurements.

References

[1] L. Tsang, J. A. Kong, and R. T. Shin, *Theory of Microwave Remote Sensing*. Hoboken, NJ: Wiley, 1985.
[2] A. Ishimaru, *Electromagnetic Wave Propagation, Radiation, and Scattering*. Englewood Cliffs, NJ: Prentice-Hall, 1991.
[3] C. S. Ruf, "Constraints on the polarization purity of a Stokes microwave radiometer," *Radio Sci.*, vol. 33, no. 6, pp. 1617–1639, Nov./Dec. 1998.
[4] S. H. Yueh, W. J. Wilson, F. K. Li, S. V. Nghiem, and W. B. Ricketts, "Polarimetric measurements of sea surface brightness temperatures using an aircraft K-band radiometer," *IEEE Trans. Geosci. Remote Sens.*, vol. 33, no. 1, pp. 85–92, Jan. 1995.
[5] J. Lahtinen, J. Pihlflyckt, I. Mononen, S. J. Tauriainen, M. Kemppinen, and M. T. Hallikainen, "Fully polarimetric microwave radiometer for remote sensing," *IEEE Trans. Geosci. Remote Sens.*, vol. 41, no. 8, pp. 1869–1878, Aug. 2003.
[6] J. R. Piepmeier, "Calibration of passive microwave polarimeters that use hybrid coupler-based correlators," *IEEE Trans. Geosci. Remote Sens.*, vol. 42, no. 2, pp. 391–400, Feb. 2004.
[7] G. Evans and C. W. McLeish, *RF Radiometer Handbook*. Dedham, MA: Artech House, 1977.
[8] J. Peng and C. S. Ruf, "Covariance statistics of polarimetric brightness temperature measurements," *IEEE Trans. Geosci. Remote Sens.*, vol. 46, no. 10, pp. 3238–3251, Oct. 2008.
[9] C. S. Ruf, C. T. Swift, A. B. Tanner, and D. M. Le Vine, "Interferometric synthetic aperture microwave radiometry for the remote sensing of the Earth," *IEEE Trans. Geosci. Remote Sens.*, vol. 26, no. 5, pp. 597–611, Sep. 1988.
[10] J. Tinbergen, *Astronomical Polarimetry*. New York: Cambridge Univ. Press, 1996.